dimensional cases difficult and in some cases impossible by other methods.

An additional advantage is that the procedure works as well in the multidimensional case, including nonlinear terms, which are then written as sums of the appropriate Adomian polynomials as discussed in Ref. 1. The procedure is also easily extended to $\nabla^2 u = f(x,y,z) + ku$ or even $\nabla^2 u + Nu = f(x,y,z) + ku$ where Nu is an analytic term.

Acknowledgment

This research was supported by AFOSR contract no. F49620-87-C-0098, with Dr. R. J. Nachman as project manager.

References

[1]Adomian, G., *Nonlinear Stochastic Operator Equations*, Academic Press, New York, 1986.

[2]Salas, M. D., Abarbanel, S., and Gottlieb, D., "Multiple Steady States for Characteristic Initial-Value Problems," Institute of Computer Applications in Science and Engineering Report, Langley Research Center, Virginia, 1986.

Numerical Evaluation of Whitham's F-Function for Supersonic Projectiles

David V. Ritzel*
Defence Research Establishment Suffield, Ralston, Alberta, Canada
and
James J. Gottlieb†
Institute for Aerospace Studies, University of Toronto, Toronto, Ontario, Canada

Introduction

IN 1952 Whitham[1] presented a nonlinear analysis accurate to first-order for determination of the complete supersonic flowfield around slender and smooth bodies of revolution, and this analysis has been used extensively to obtain flowfields about supersonic projectiles, missiles, and aircraft. At the center of this analysis is his F-function

$$F(y) = \frac{1}{2\pi}\int_0^y \frac{A''(x)}{\sqrt{y-x}}\,dx \tag{1}$$

where $A(x)$ defines the cross-sectional area of the body with axial distance x measured from the body nose, and $A''(x)$ is its double derivative. Whitham's variable y defines the origin of a characteristic curve emanating from the body surface, by being equal to $x-\beta r$ at the surface, where $\beta = (M_\infty^2 - 1)^{1/2}$. Physically, this is the axial distance from the body nose to a point at which a characteristic curve, when extended backward from the surface, intersects the x axis. For more complex bodies such as aircraft, $A(x)$ may be considered as an effective cross-sectional area that includes lift and other effects.

In using Whitham's analysis, it is obvious that much of the work is centered on determining $F(y)$ by integration. If the cross-sectional area of the body is an extremely simple function of distance, then $F(y)$ may be obtained by analytic integration. The shapes of real projectiles, missiles, and aircraft, however, are normally too complicated for analytic integrations, and one must resort to a numerical integration procedure.

Carlson[2] developed a numerical integration procedure that has been used since the 1960s. In this method the body is subdivided into many segments of equal or unequal lengths. The area variations of these segments are modeled as a series of piecewise, continuous, parabolic arcs. In this case, $A''(x)$ is a constant for each segment, and the piecewise analytic integrations to obtain $F(y)$ can be done easily, constituting the major advantage of this method.

A variation of Carlson's scheme was introduced by Igoe,[3] primarily to improve accuracy of the numerical integration. Igoe's procedure uses more accurate second derivatives than Carlson's method. They are obtained from central-difference formulas of finite-difference techniques, which are based on early mathematical work of Richardson.[4] Although this method is more accurate than Carlson's, it is more difficult to use and also requires that the body be subdivided into numerous short segments of equal size. Furthermore, Richardson's extrapolation technique must be used with caution to avoid numerical difficulties for very short segments.

This paper presents an accurate and efficient numerical method for evaluating $F(y)$. It is as accurate as Igoe's method, presents no computational difficulties, and reveals physical insight on how particular body shape features contribute to the $F(y)$. It is more difficult, however, to program in computers than either Carlson's or Igoe's methods.

Numerical Evaluation of $F(y)$

The body is subdivided into a series of segments, normally of unequal lengths, so that any simple-shaped section of arbitrary length can be included efficiently as a single segment. Furthermore, a segment may arbitrarily be made short to closely model a particular, complex part of the body shape, without forcing a subdivision of other segments, as illustrated in Fig. 1a. These modeling features can markedly reduce the total number of body segments compared to the methods of Carlson[2] and Igoe.[3] In the present work the ith segment of a body has a radius given by

$$R_i(x) = \sum_{j=0}^{n_i} a_{i,j}[x - x_i]^j$$

which is a polynomial curve with a finite number of terms (n_i normally less than 5). The sequence of polynomial segments representing the entire body shape is usually piecewise continuous in position and slope at the junctions between segments. For the ith segment this defines the coefficients $a_{i,j}$ for $0 \le j \le n_i$, and for convenience the coefficients $a_{i,j}$ for $n_i < j \le 2n_i$ are set equal to zero.

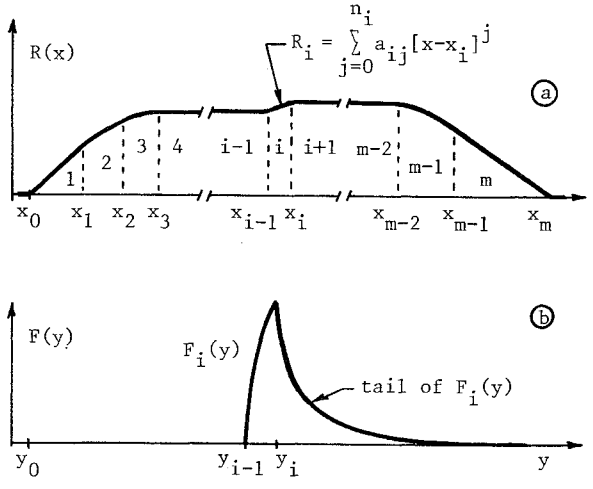

Fig. 1 Body shape defined by m piecewise polynomial segments (a) and the contribution of the ith body segment to the F-function (b).

Received April 15, 1987; revision received June 15, 1987.

*Defense Scientist.

†Associate Professor.

From the previous polynomial form of $R_i(x)$, one can show that the body area

$$A_i(x) = \pi \sum_{j=0}^{2n_i} b_{i,j}[x-x_i]^j \tag{2}$$

where the coefficients

$$b_{i,j} = \sum_{k=0}^{j} a_{i,k}a_{i,j-k} \tag{3}$$

and

$$A_i''(x) = \pi \sum_{j=0}^{2n_i-2} c_{i,j}[x-x_i]^j \tag{4}$$

where

$$c_{i,j} = (j+2)(j+1)\sum_{k=0}^{j+2} a_{i,k}a_{i,j-k+2} \tag{5}$$

This illustrates that polynomial curves fitted to the body shape $R(x)$ also result in polynomial representations of body area $A(x)$ and its derivatives, although the degree of these polynomials is different. For a polynomial curve-fit to $R_i(x)$ of degree n_i, the degree of the polynomial for $A_i''(x)$ is $2n_i-2$.

The integral for the ith body segment and ith part of the F-function, denoted as $F_i(y)$, may be integrated analytically, because $A_i''(x)$ is a simple polynomial. This integration may be done systematically by parts, where the term with $y-x$ is integrated and the polynomial is differentiated. By continuing this integration by parts until the polynomial parts have been eliminated, and then inserting the integration limits, the solution for $F_i(y)$ can be obtained. When all $F_i(y)$ have been determined in this manner, the total solution is

$$F(y) = \sum_{i=1}^{m} F_i(y) = \sum_{i=1}^{m} f_i(y,y_{i-1})H\{y-y_{i-1}\}$$
$$-f_i(y,y_i)H\{y-y_i\} \tag{6}$$

for all m segments where

$$f_i(y,z) = \sum_{j=0}^{2n_i-2} \frac{2^{2j+1}j!}{(2j+1)!} G_i^j(z)[y-z]^{j+\frac{1}{2}} \tag{7}$$

$$G_i(x) = \frac{1}{2\pi} A_i''(x) = [R_i'(x)]^2 + R_i(x)R_i''(x) \tag{8}$$

$$G_i^j(z) = \frac{d^j}{dx^j} G_i(x)\Big|_{x=z'} \tag{9}$$

and $H\{\ \}$ is Heaviside's unit step function.

From this solution for $F(y)$ one can clearly see that the contribution of any segment may be isolated, in analytical form if necessary. If this is done, it is evident that the ith contribution of $F(y)$ from $F_i(y)$ has two distinct parts according to Eqs. (6) and (7) (illustrated in Fig. 1b). The first part usually increases (or decreases) from zero to a final value during the interval $y_{i-1} \le y \le y_i$, and the second part always decays from this final value back to zero for $y \ge y_i$. This decaying part is called the tail.

Although the previous solution for $F(y)$ is elegant and useful, computer evaluations of the tail of $F_i(y)$ for $y \gg y_i$ lead to numerical difficulties, because the continuously decaying tail involves the subtraction of two diverging functions whose difference slowly approaches zero with increasing y. For example, if $n_i = 1$ so that $A_i''(x)$ is constant, the tail function is then given by $(2A_i''/\pi)\ [(y-y_i)^{\frac{1}{2}} - (y-y_{i-1})^{\frac{1}{2}}]$ for $y > y_i$. This problem is more acute for higher-order polynomials, shorter segments, and computers having fewer significant digits.

To eliminate this difficulty and to make the method useful in general, the following procedure is used. The tail of $F_i(y)$ is given by $f_i(y,y_{i-1}) - f_i(y,y_i)$ from Eq. (6) (for $y \ge y_i$). In the last term $f_i(y,y_i)$ a factor given by $[y-y_i]^{j+\frac{1}{2}}$ [Eq. (7)] may be rearranged to have the form

$$[y_i - y_{i-1}]^{j+\frac{1}{2}} \eta^{-j-\frac{1}{2}} [1-\eta]^{j+\frac{1}{2}}$$

where

$$\eta = [y_i - y_{i-1}]/[y-y_{i-1}]$$

Since η always has values in the range from 0 to 1 for $y \ge y_i$, the term $[1-\eta]^{j+\frac{1}{2}}$ may be expanded by using the binomial theorem. Each expansion has an infinite number of terms, but there are only $2n_i - 1$ of these expansions—one for each term in the series of $A_i''(x)$. The next step is to regroup all terms of the difference $f_i(y,y_{i-1}) - f_i(y,y_i)$ to form a descending series in terms of the powers of η.

Each term of these $2n_i - 1$ series contains a mix of $G_i^j(y_{i-1})$ and $G_i^j(y_i)$ or simply $G_i^j(y_i)$ as a factor. However, $G_i(y_{i-1})$ and $G_i(y_i)$ and their derivatives are immediately related. For example, if $n_i = 2$ then the polynomial equation for $G_i'(y)$ may be expressed as

$$G_i(y_i) + G_i'(y_i)[y-y_i] + (1/2)G_i''(y_i)[y-y_i]^2$$

and this at length leads to

$$G_i(y_{i-1}) = G_i(y_i) - G_i'(y_i)[y_i - y_{i-1}] + G_i''(y_i)[y_i - y_{i-1}]^2$$

$$G_i(y_{i-1}) = G_i'(y_i) - G_i''(y_i)[y_i - y_{i-1}]$$

and

$$G_i''(y_{i-1}) = G_i''(y_i)$$

With these relationships one may show that all terms from $f_i(y_{i-1})$ in the expanded tail function $f_i(y_{i-1}) - f_i(y_i)$ will cancel from the $2n_i - 1$ series. This cancellation also results in disappearance of all terms involving η with negative powers, as required for a convergence series to be well behaved. Although this cancellation and rearrangement process is extremely tedious, the final results for $F_i(y)$ for the tail ($y \ge y_i$) may be summarized as

$$F_i(y) = \sum_{j=0}^{2n_i-2} (-1)^j G_i^j(y_i)(y_i - y_{i-1})^{j+\frac{1}{2}} T(j,\eta) \tag{10}$$

where

$$T(j,\eta) = \sum_{k=0}^{\infty} \frac{(2k)!\eta^{k+\frac{1}{2}}}{4^k k!(j+k+1)!} \tag{11}$$

In this form the remainder of the $2n_i - 1$ infinite series appears as a family of generalized functions denoted by $T(j,\eta)$. These infinite series have good convergence properties and are therefore well behaved computationally.

This completes the solution for evaluating the integral of Eq. (1) to get $F(y)$. For each $F_i(y)$ one uses Eqs. (6–9) for the range $y_{i-1} \le y \le y_i$, and Eqs. (8–11) for the range $y > y_i$. These equations will be well behaved computationally for bodies' shapes modeled with equal or unequal segments of arbitrary length. The function $T(j,\eta)$ can be calculated each time they are needed in a computer program, because the computations require very little CPU time. They can also be computed just once and replaced by suitable curve fits since they are independent of the body shape. The first five normalized $T(j,\eta)$ functions are shown in Fig. 2.

Numerical Results

Figure 3 depicts a hypothetical body with a simple slender and smooth shape, the body radius $R(x)$ and the resulting

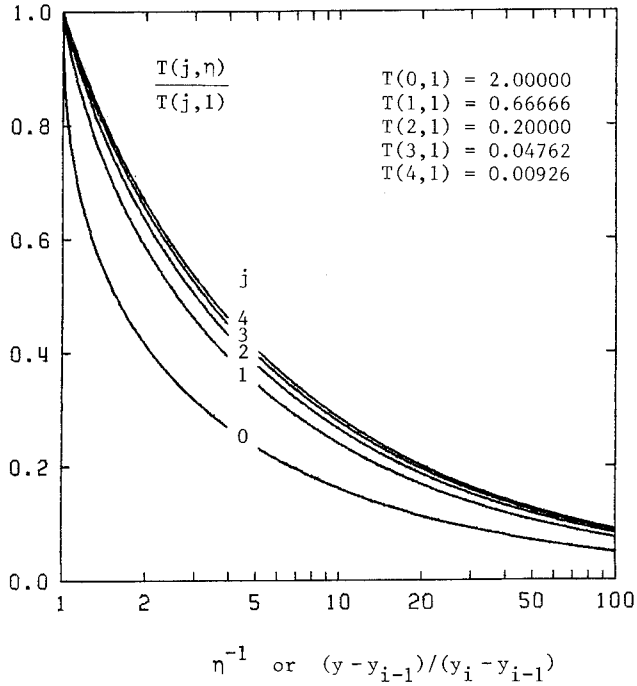

Fig. 2 First five normalized functions of $T(j,\eta)$.

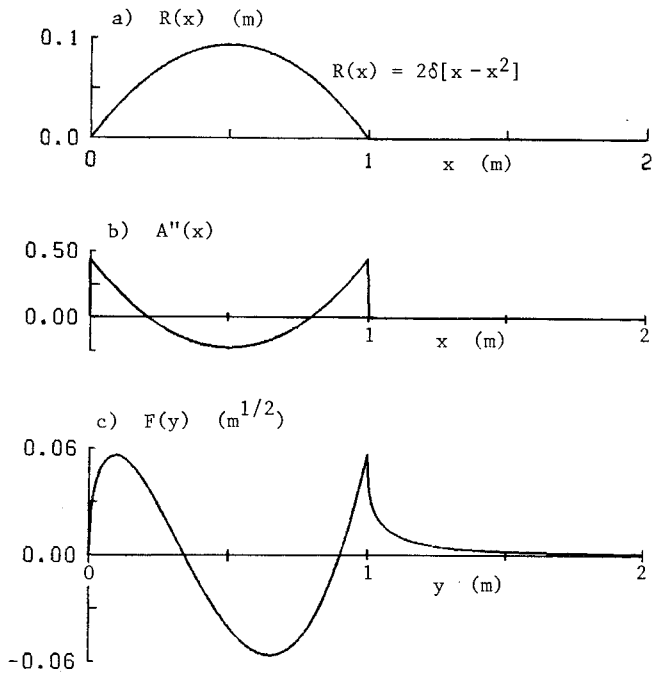

Fig. 3 $R(x)$, $A''(x)$ and $F(y)$ for a parabolic-arc-shaped body.

$A''(x)$ and $F(y)$ with the body length of 1 m and a thickness ratio $\delta = 0.1875$. When this body is subdivided into 15 segments of equal length the resulting F-functions for the individual segments from the previous analysis are shown in Fig. 4. The complete F-function in Fig. 3c will be obtained when these functions are summed.

The final example is a military projectile with a nominal diameter of 7.6 cm and length of 41 cm. The projectile has an ogival nose with conical mid-nose section followed by a rounded shoulder to the main cylindrical body, as shown by the body radius $R(x)$ in Fig. 5a. The rear of the cylinder has a slight boat-tail followed by a flat base (vertical dashed line). The inverted cone attached to the base (after the dashed line) is the wake being modeled as a solid afterbody.

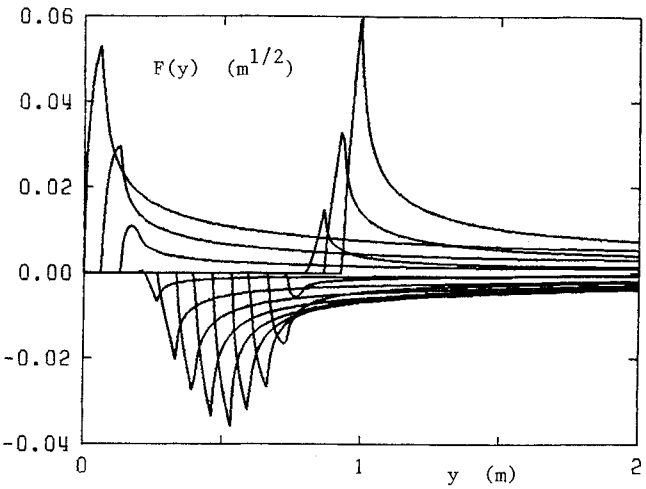

Fig. 4 15 F-functions from equal length segments of a parabolic-arc-shaped body, which will give $F(y)$ in the previous figure when added.

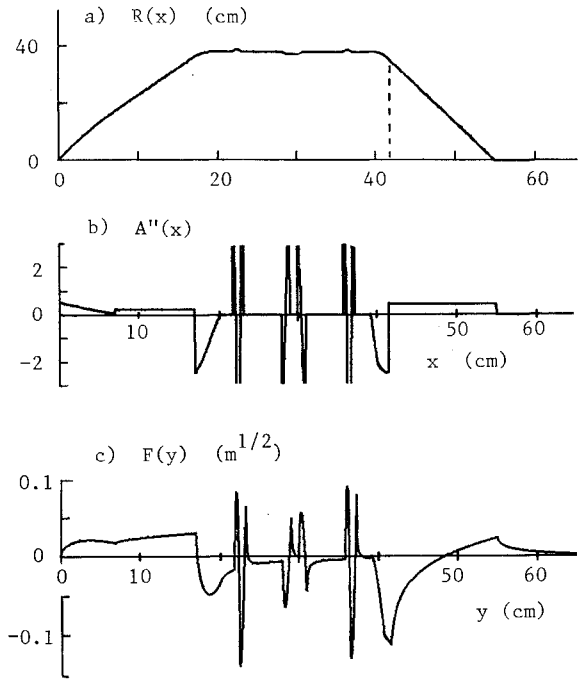

Fig. 5 $R(x)$, $A''(x)$ and $F(y)$ for a free-flight projectile ($D = 7.6$ cm, $L = 41$ cm).

Barely noticeable in $R(x)$ are two small bumps or ridges and a shallow groove located at distances of 22, 29, and 36 cm from the nose. Each has a curved front and back and differs by about 2% from the nominal body radius. Note that such bumps on actual projectiles are often the driving bands that help center the projectile in the barrel and provide a seal to minimize leakage of propellant gases past the projectile. Although these bumps are barely noticeable in the profile of $R(x)$, their high curvature is pronounced in $A''(x)$ given in Fig. 5b. The peaks of some of these spikes reach values of ± 8 and have been clipped to save space.

This body was subdivided into 16 unequal length segments to obtain the F-function shown in Fig. 5c. For example, the nose front consists of three segments, the bumps and boat-tailed rear each have two, and the groove consists of three segments because the central part is of constant area. All other segments are of constant area and therefore do not contribute to $F(y)$. Because of the high local body curvature

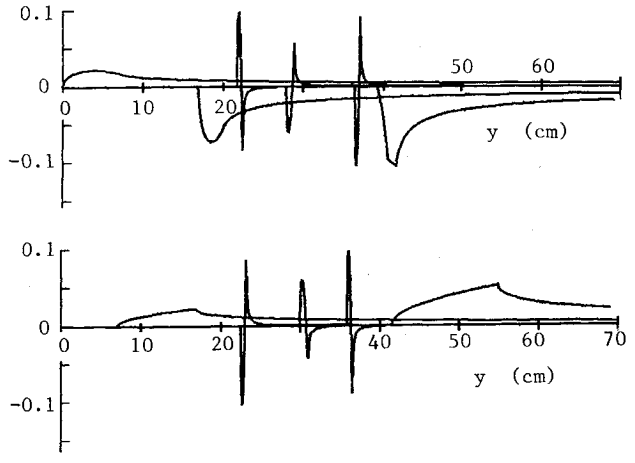

Fig. 6 Individual F-functions from unequal length segments for a free-flight projectile ($D=7.6$ cm, $L=41$ cm).

at the bumps and groove, $F(y)$ is spiky, characteristic of actual projectiles.

The F-functions from individual segments are depicted in Fig. 6. For clarity about half of them are shown at the top and the others appear at the bottom. The contributions from the bumps and groove are interesting. The front of a bump produces a short N-shaped contribution and the rear produces an inverted N-shaped addition. These occur in reverse order for a groove. Such individual contributions are not so apparent in the full $F(y)$ of Fig. 5c.

Acknowledgments

Funding from the Defence Research Establishment Suffield, Ralston, Alberta, Canada, and the Natural Sciences and Engineering Research Council of Canada is acknowledged with appreciation.

References

[1]Whitham, G. B., "The Flow Pattern of a Supersonic Projectile," *Commun. Pure and Applied Math.*, Vol. 5, 1952, pp. 301-348.

[2]Carlson, H. W., "Influence of Airplane Configurations on Sonic-Boom Characteristics," *Journal of Aircraft*, Vol. 1, 1964, pp. 82-86.

[3]Igoe, W. B., "Application of Richardson's Extrapolation to Numerical Evaluation of Sonic-Boom Integrals," NASA TN D-3806, March 1967.

[4]Richardson, L. F., "The Approximate Arithmetical Solution by Finite Differences of Physical Problems Involving Differential Equations, with an Application to the Stresses in a Masonary Dam," Phil. Trans. Roy. Soc. London, Ser. A, Vol. 210, No. 467, 1910, pp. 307-357.

Poisson-Kirchhoff Paradox in Flexure of Plates

K. Vijayakumar*
Indian Institute of Science, Bangalore, India

Introduction

In a recent article[1] that various plate theories (including his own notable contributions) concerning the Poisson-Kirchhoff boundary conditions paradox, Reissner remarked that the problem of modifying Kirchhoff's approximations of the displacements for an improved sixth-order plate theory has not been completely resolved. He expected that a sixth-order differential equation governing the deflection $w_0(x,y)$ might be of the form $D\nabla^2\nabla^2 w_0 - C\nabla^2\nabla^2\nabla^2 w_0 = q$, with some suitable factor function C. However, no way of finding this equation has been offered until now. In the present work, it is shown that the key to deriving such an equation lies in Reissner's aforementioned remark, with only one slight alteration. Instead of displacements, we direct our attention to the problem of modifying Kirchhoff's assumptions with regard to transverse normal and shear strains.

An iterative scheme is presented here through which an assumed state of transverse normal and shear strains can be transformed into a new state by integration of strain-displacement relations and equilibrium equations. Starting with Kirchhoff's assumptions, the iterative process is carried out to develop expressions for displacements and stresses. In the limit, each of these expressions is in the form of an infinite series in which each term is a product of a known function of thickness coordinate z and a differential expression involving mid-plane deflection $w_0(x,y)$. The expressions thus obtained for displacements and stresses satisfy all field equations for arbitrary function $w_0(x,y)$. By taking the first two terms in the series for normal stress σ_z and satisfying the surface load condition, it is shown that the plate behavior is governed by a sixth-order differential equation involving $w_0(x,y)$. It is indeed, in the form as expected by Reissner.

Analysis

For simplicity in presentation, a rectilinear domain $0\le x\le a$, $0\le y\le b$, and $-h\le z\le +h$ with reference to Cartesian coordinate system x,y,z is considered. The thickness $2h$ of the plate is small compared to its lateral dimensions a and b. The material of the plate is homogeneous and isotropic with elastic constants E (Young's modulus), ν (Poisson's ratio), and G (modulus of rigidity) that are related to each other by $E=2(1+\nu)G$.

The plate is subjected to asymmetric load $q(x,y)$ along top and bottom surfaces ($z=\pm h$). We assume that the boundary conditions along the edges are prescribed so that the in-plane displacements (u,v) and bending stresses $(\sigma_x,\sigma_y,\tau_{xy})$ are antisymmetric in z and the normal deflection w and transverse shear stresses (τ_{xz},τ_{yz}) are symmetric in z. We treat the problem within the classical small deformation theory of three-dimensional elasticity.

In the iterative scheme envisaged here, Kirchhoff's assumed state of strains is expressed as

$$\epsilon_z^{(0)}=0, \qquad \gamma_{xz}^{(0)}=0, \qquad \gamma_{yz}^{(0)}=0 \tag{1}$$

Let $\epsilon_z^{(i)}$, $\gamma_{xz}^{(i)}$, and $\gamma_{yz}^{(i)}$ be the transverse normal and shear strains at the ith stage of iteration. By substituting in strain-displacement relations,

$$\epsilon_z=\frac{\partial w}{\partial z}, \qquad \gamma_{xz}=\frac{\partial u}{\partial z}+\frac{\partial w}{\partial x}, \qquad \gamma_{yz}=\frac{\partial v}{\partial z}+\frac{\partial w}{\partial y}$$

integrating with respect to z and using the assumed symmetries in the problem, one obtains the displacments in the form

$$w^{(i)}=w_0(x,y)+\int_0^z \epsilon_z^{(i)}\,dz \tag{2}$$

$$u^{(i)}=-\frac{\partial}{\partial x}\left[zw_0+\int_0^z\int_0^z \epsilon_z^{(i)}(dz)_2\right]+\int_0^z \gamma_{xz}^{(i)}\,dz \tag{3}$$

and a similar expression for $v^{(i)}$.

Received Dec. 29, 1986; revision received March 11, 1987.

*Associate Professor, Department of Aerospace Engineering.